Monthly Simulation of Surface Layer Fluxes and Soil Properties during FIFE

MICHAEL G. BOSILOVICH* AND WEN-YIH SUN

Department of Earth and Atmospheric Sciences, Purdue University, West Lafayette, Indiana

(Manuscript received 9 April 1996, in final form 3 April 1997)

ABSTRACT

Global change and regional climate experiments with atmospheric numerical models rely on the parameterization of the surface boundary in order to evaluate impact on society and agriculture. In this paper, several surface modeling strategies have been examined in order to test their ability to simulate for a period of one month, and hence, their impact on short-term and regional climate modeling. The interaction between vegetation and soil models is also discussed. The resolution of a multiple-level soil model, the method of computing moisture availability, the Force–Restore Method, and vegetation parameterization were studied by comparing model-simulated soil temperature, soil moisture, and surface energy budget with observations and intercomparison of the simulations.

The increase of model soil resolution improved both the simulation of daytime ground heat flux and latent heat. Evaporation from the soil surface with more coarse resolution soil was larger than the higher resolution simulation, but transpiration and the simulation of soil water were similar for each case. The Alpha method of moisture availability allowed less soil evaporation under stressed conditions than the Beta method. The soil water became larger than the observations, and more transpiration occurred. The Force–Restore Method simulations produced reasonable results, when coupled with the vegetation model. Eliminating the vegetation model from several of the previous cases, however, produced significant variability between different soil models. It is possible that this variability could affect long-term GCM sensitivity simulations.

1. Introduction

Many studies have shown that surface properties influence meteorology at climate, synoptic, and local time and space scales. In an effort to account for these influences, surface models that include parameterizations of the detailed physics are incorporated into atmospheric numerical models (Dickinson 1984; Sellers et al. 1986; and many others). Currently, regional hydrologic budgets are being studied using limited-area numerical models for time periods ranging from a month to years (Giorgi et al. 1992; Paegle et al. 1996). The numerically modeled regional hydrologic cycle and climate should depend greatly on the ability of the surface model to simulate boundary processes, and model validation for longer periods is necessary (Betts et al. 1993; Garrat 1993). Beljaars et al. (1996) demonstrate that the proper initialization and simulation of soil water can improve the prediction of precipitation in an atmospheric numerical model.

Kondo et al. (1992) studied different soil models over long time periods (7–150 days). Model results indicated that different parameterizations of deep soil processes can cause significant differences in modeled evaporation in as little as 10 days. Because surface evaporation is a key element of the regional hydrology budget, it is very important that the surface parameterization simulate reliable soil moisture and evaporation for the long periods used in the study of climate. Furthermore, Kondo et al. (1992) used 25 layers in the soil model. While more layers should provide a more accurate result, using too many layers is not feasible in three-dimensional atmospheric numerical models, given the limitation of current computer technology. Many atmospheric models consider three or four layers of soil, where soil moisture and temperature are predicted. It may be useful to quantify the impact of coarser resolution simulations on the surface energy budget. Also, the parameterization of moisture availability of the soil surface is an important component of the computation of evaporation, but a generalized formulation is difficult to identify (Mahfouf and Noihlan 1991; Dekić et al. 1995). The presence of vegetation at the surface should be a very important boundary condition, but its sensitivity to different soil processes is not clearly defined (Mihailović et al. 1992; Sun and Bosilovich 1996).

Bosilovich and Sun (1995) presented the formulation of a surface model intended for use in atmospheric nu-

*Current affiliation: Universities Space Research Association, NASA/Goddard Space Flight Center, Greenbelt, Maryland.

Corresponding author address: Michael G. Bosilovich, Universities Space Research Association, NASA/Goddard Space Flight Center, Greenbelt, MD 20771.
E-mail: mikeb@dao.gsfc.nasa.gov

merical models. The surface model was validated with surface-layer turbulent fluxes and soil temperatures for three cases with periods of 40 hours (two days and one night). The period of simulation was adequate for PBL and mesoscale modeling studies (Sun and Bosilovich 1996; Sun and Chern 1993); however, the variations of deep soil processes are minimized over this short simulation. The present study will adopt similar methodology as Bosilovich and Sun (1995) in that ''stand alone'' surface simulations are performed to test the ability of the model. The duration of the simulation is extended in an effort to examine the ability of the model to simulate soil processes over the longer periods of time that accompany the simulation of regional climate heat and moisture budgets in both limited domain and general circulation models.

The main purpose of this work is to identify the ability of the land surface parameterization to simulate deep soil temperature, soil moisture, and surface fluxes for periods up to one month and to identify any bias or weaknesses present in the model compared to observational data and other modeling options. Observational data used to verify the numerical simulations is derived from the First ISLSCP Field Experiment (FIFE) (Sellers et al. 1988; Strebel et al. 1994) and is discussed in the following section and appendix A. Section 3 will include a brief discussion of the models and the methodology of the experiments. Model results and conclusions are presented in sections 4 and 5, respectively.

2. Observational data

All observational data utilized in these experiments were obtained from the Betts and Ball (1998) FIFE site average dataset. The site average atmospheric temperature, moisture, wind, component radiative fluxes and pressure are used to drive the model simulation, as in Sellers and Dorman (1987), Smith et al. (1993), and Bosilovich and Sun (1995). The most detailed observations were taken during Intensive Field Campaigns (IFCs), which lasted approximately two weeks each. Some automated stations, however, continued recording data beyond the IFCs. For the experiments presented here the simulation period is 1045 UTC 25 June 1987, roughly the beginning of FIFE's IFC 2, and continues through 25 July 1987. The model also requires the net shortwave and downward longwave radiation components of net radiation as input. While these data are available, a well-documented bias between the directional radiometers and net radiometers exists in the FIFE archives (Smith et al. 1992; Field et al. 1992). Ultimately this will have some impact on the verification of the model. A correction has been applied to the surface energy balance. Details of the correction are discussed in appendix A.

The Betts and Ball (1998) dataset also includes site-averaged soil temperature and soil moisture data that will be used to initialize and verify the model simulations. During IFC 2 gravimetric soil moisture was observed (0–10-cm depth) each day at several sites, but only about once per week between IFCs. Neutron probe measurements, which extended to 2-m depth at some sites, were made approximately once per week (Ungar et al. 1992; Wang 1992). The soil moisture observations were site averaged, then interpolated to fill in missing days between IFCs to provide a continuous daily record (Betts and Ball 1998). Betts and Ball discuss the reliability of the neutron probe data. They find an imbalance between the vertically integrated change of soil water content and the surface measurements of evaporation and precipitation. This suggests that the soil moisture measurements have some weaknesses; however, for this study, the soil moisture observations will be utilized as initial conditions for the model simulation.

TABLE 1. Boundary conditions and model constants. The soil type is used to specify several constants related to the soil texture: z_{og} is the roughness length of bare soil, ϵ_g is the emissivity of the soil surface, σ_f is the fraction of vegetation cover, h_c is the canopy height, LAI is the leaf area index, R_{smin} is the minimum stomatal resistance of the canopy, and ϵ_f is the emissivity of the vegetation canopy.

Soil type	z_{og} (m)	ϵ_g	σ_f	h_c (m)	LAI ($m^2\ m^{-2}$)	R_{smin} ($s\ m^{-1}$)	ϵ_f
Silty clay loam	0.05	0.96	0.80	0.50	1.30	125.00	0.90

Wherever possible, observations were used to provide the boundary and initial conditions in the model (Table 1). FIFE provides detailed estimates of other boundary data required for model simulation, such as vegetation cover and height, leaf area index, soil texture, and vegetation type. For vegetation properties of leaf area index and vegetation height, data for all available sites was obtained from the FIFE CD-ROM (Strebel et al. 1994) and averaged for the FIFE domain. Unfortunately, some observations were made no more frequently than once per month. No effort was made to change these values in time, although it is recognized that on the timescale of the simulation, these values are not constant.

3. Methodology

a. Model

The model utilized in this work has been described in detail by Bosilovich and Sun (1995) and further sensitivity tests were performed by Sun and Bosilovich (1996); therefore, only a brief description of the model and experimental design will be presented. The surface model will be run in a stand alone fashion in that reference level input data are derived from observations. The data used for input consists of atmospheric reference level (5.4 m) wind speed, air temperature at 2 m, specific humidity at 2 m, surface pressure, precipitation, and incoming longwave and net shortwave radiation. These observations are reported at 30-min intervals. Soil temperature and moisture are also derived initially from the observational dataset, but are predicted by the model

TABLE 2. Soil model structure and initialization for the Bosilovich and Sun (1995) model with eight and five layers and the FRM surface and bulk layers: Z is the midpoint depth of the layer, ΔZ is the thickness of the soil layer, w is the initial volumetric soil water content, T is the initial soil temperature, λ is the soil thermal conductivity, and c_{et} is the root fraction. Note that for the FRM Z and ΔZ are for the soil moisture prediction equation, the soil temperature equations use variable thicknesses.

Layer	Z (m)	ΔZ	w (m^3m^{-3})	T (K)	λ (W m^{-1} K^{-1})	C_{et}
1	0.005	0.01	0.357	289.0	1.1	0.00
2	0.020	0.02	0.357	290.0	1.1	0.00
3	0.050	0.04	0.352	293.0	1.1	0.15
4	0.100	0.06	0.360	296.0	0.6	0.30
5	0.200	0.14	0.370	296.0	0.2	0.30
6	0.500	0.46	0.370	295.2	0.2	0.25
7	0.990	0.52	0.370	295.2	0.2	0.00
8	1.625	0.75	0.380	295.2	0.2	0.00
1	0.025	0.05	0.350	290.0	1.1	0.10
2	0.175	0.25	0.370	295.2	0.2	0.70
3	0.500	0.40	0.370	295.2	0.2	0.20
4	1.000	0.60	0.370	295.2	0.2	0.00
5	1.650	0.70	0.380	295.2	0.2	0.00
			FRM			
1	0.05	0.10	0.370	288	1.1	0.20
2	1.000	2.00	0.370	295.2	0.2	0.80

after the initial time. The initial conditions for the soil model of all simulations are provided in Table 2. The model is integrated at a time interval of 60 s, and the forcing data are linearly interpolated to this interval. The soil model, based on the simplified formulation of Philip (1957) (see also Sellers et al. 1986; Kondo et al. 1992), however, has been modified so that more than three model layers can be considered. Primarily, this was done so that certain model grids can be created to coincide with observations at different depths. Higher resolution soil grids are employed here to define differences between fine and coarse resolution grids. The variable grid will also be useful in the future, when computational limitations in three-dimensional modeling will not be as restrictive. The method of computing moisture availability and the Force–Restore Method (FRM) for prediction of soil water and temperature will be tested in the model simulation. The hydrological parameters that define the soil texture (in this case, silty clay loam) are given by Clapp and Hornberger (1978). Some specifics of these parameterizations and the computation of model evapotranspiration will be discussed further.

1) MOISTURE AVAILABILITY

To compute evaporation from the soil surface, knowledge of the specific humidity gradient between the land surface and atmosphere is essential. Soil surface specific humidity is generally not predicted, and it is difficult to measure in the field. Therefore, many parameterizations have been developed to close the evaporation equation. Unfortunately, no single method seems to be generally applicable to all cases, as evidenced by conflicting results in numerous experiments [see Mahfouf and Noihlan (1991) and Dekić et al. (1995) for a complete review].

The method of Noihlan and Planton (1989) was originally employed because of the reasonable results over many different case studies (Noihlan and Planton 1989; Jacquemin and Noihlan 1990; Braud et al. 1993; Bosilovich and Sun 1995). Mahfouf and Noihlan verified the method by intercomparing several models and observed soil water content and cumulative evaporation. Noihlan and Planton's Alpha method computes soil surface specific humidity (q_g) by

$$q_g = \alpha q_s(T_g),$$

where

$$\alpha = \begin{cases} \dfrac{1}{2}\left[1 - \cos\left(\pi \dfrac{w_g}{w_{\rm fc}}\right)\right], & w_g < w_{\rm fc} \\ 1.0, & w_g \geq w_{\rm fc}. \end{cases} \quad (1)$$

In (1), $w_{\rm fc}$ is the field capacity of the soil, w_g is the soil water content of the surface soil layer, and T_g is the temperature of the top soil layer: α can be thought of as the relative humidity of the soil surface. All variables are defined in appendix B.

Recently, Dekić et al. (1995) studied several different methods of computing the soil surface specific humidity and found that the Noihlan and Planton (1989) method produced a serious underestimation of latent heat flux during moderately dry conditions. Dekić et al. results indicate that the method introduced by Deardorff (1977, 1978) produced some of the least biased values of latent heat flux from bare soil. This is most surprising, considering the simplified linear nature of the parameterization. Deardorff's surface specific humidity (Beta method) is computed by

$$q_g = \beta q_s(T_g) + (1 - \beta) q_a,$$

where

$$\beta = \begin{cases} w_g / w_{\rm fc}, & w_g < w_{\rm fc} \\ 1.0, & w_g \geq w_{\rm fc}. \end{cases} \quad (2)$$

When considered with the equation that computes actual evaporation, β is related to the moisture availability parameter utilized by many models. A comparison between model simulations using the two methods will be presented. While Dekić et al. separated moist and dry cases, their simulations were of a shorter duration and did not include a vegetation-covered surface. We will be able to expand their results by also comparing modeled soil moisture with observations and by intercomparing the impact on modeled transpiration.

2) FORCE–RESTORE METHOD

It is also worthwhile to investigate the use of even more simplified soil parameterizations, in the interest of computational efficiency. The FRM (Blackadar 1976; Bhumralkar 1975; Deardorff 1977, 1978) has been a popular and efficient model for predicting soil moisture and temperature. The FRM soil parameterization consists of two parts: a bulk soil layer for both heat and water, analogous to the ''bucket model'' of Manabe (1969), and a top thin layer intended to estimate values of surface soil water and temperature in order to provide more reliable values at the boundary. The FRM soil temperature equations have performed very well in idealized studies as compared to analytical solutions (Yee 1988; Dickinson 1988; Savijärvi 1992). Similar studies have not been performed for the soil water equations. The soil water prediction problem is somewhat different than that for temperature in that the mass of water is passing through the mass of soil. Forces other than diffusion, such as gravity, can affect the movement of the mass of water. Soil density and soil hydraulic properties become very important in this process. Complicating the process is the fact that the hydraulic properties are functions of the soil water itself and there is some uncertainty as the water content approaches zero (Clapp and Hornberger 1978). The FRM as discussed by Deardorff will be applied, in place of the soil temperature and moisture prediction equations employed by Bosilovich and Sun (1995), to test its ability, compared to observations.

The FRM soil moisture prediction equations are

$$\frac{\partial w_g}{\partial t} = -C_1\frac{E_g + C_{\text{et1}}E_{\text{tr}} - P_g}{\rho_w d_1} - C_2\frac{w_g - w_2}{\tau_1} \quad (3)$$

$$\frac{\partial w_2}{\partial t} = -\frac{E_g + E_{\text{tr}} - P_g}{\rho_w d_2}. \quad (4)$$

The first term on the right-hand side is the net flux of water between the soil and atmosphere; C_1 is a function of the surface soil water content (w_g), which increases as soil moisture decreases; E_g is the soil surface evaporation; P_g is the amount of precipitation permitted to infiltrate the soil; E_{tr} is the total amount of transpiration of the vegetation canopy; C_{etl} is the root fraction of the topsoil layer. The restoring term is second on the right-hand side; C_2 is a constant; and τ_1 is a time constant equal to the diurnal period. Note that, in these equations, depths d_1 and d_2 are constants (10 cm and 2 m, respectively), whereas the corresponding depths in the FRM temperature prediction equations are variable, dependant on the soil moisture and thermal conductivity. Deardorff (1978) notes that the depths in the soil moisture equations should be variable, but the variability has been absorbed into the C_1 coefficient, which is a function of surface soil water content.

Deardorff (1978) derived C_1 and C_2 based on observation at one observing station, yet his formula has been adopted by many as a generalization. The linear function for C_1 is

$$C_1 = \begin{cases} 0.5, & w_g \geq w_{\text{fc}} \\ 14 - 16.875(w_g/w_{\text{fc}} - 0.2), & w_{\text{fc}} > w_g > 0.2w_{\text{fc}} \\ 14, & w_g \leq 0.2w_{\text{fc}}. \end{cases} \quad (5)$$

The value for C_2 is a constant set at 0.9. This method will be referred to as D78 in the text. Note that when the soil is dry, C_1 becomes large and amplifies the value of $E - P$. Noihlan and Planton (1989) and Braud et al. (1993) derive more generalized parameterizations of C_1 and C_2, based upon Clapp and Hornberger (1978) soil texture and diffusion of soil water through the soil. The Braud et al. (1993) formulation of C_1 and C_2 is given by

$$C_1 = 2d_1\sqrt{\frac{\pi c_w}{\tau(K_1 + D_{vh}/\rho_w)}} \quad (6)$$

and

$$C_2 = C_{2\text{ref}}\frac{w_2}{w_{\text{sat}} - w_2 + w_1}, \quad (7)$$

where D_{vh} represents the vapor phase diffusion of soil water, which is a function of the soil texture; K_1 is the hydraulic conductivity of the soil and is computed as a function of soil water content and soil texture. Other variables are defined in appendix B. This method will be referred to as B93 in the text. Specifics on this computation of C_1 and C_2 are provided by Braud et al.

Care must be taken when interpreting the FRM soil moisture. The bulk soil water content w_2 is the mean soil water for the whole soil column. The surface soil water content w_g represents near-surface soil water that is not related to a soil layer of constant thickness [d_1 cancels when Eq. (6) is substituted into Eq. (3)]. The primary advantages of the FRM are its computational efficiency and simple input values. The Braud et al. model, however, requires a substantial increase in both input variable and computations to calculate C_1 and C_2.

3) EVAPOTRANSPIRATION

The model explicitly computes evaporation for the soil surface, vegetation surface, and transpiration. The actual model evaporation depends on the gradient of moisture between both vegetation and ground surfaces and the atmosphere, wind speed in the surface layer, and the turbulent intensity of the surface layer. The atmospheric surface layer is assumed to be a constant flux layer, which permits the use of similarity theory (Bus-

inger et al. 1971) to compute turbulent fluxes. Total surface evaporation can be written as a function of scaling variables,

$$E = -\rho u_* q_*, \tag{8}$$

or with mean gradients and the turbulent transfer coefficient,

$$E = \rho C_H U_a (q_{\text{sfc}} - q_a) \tag{9}$$

(all variables are defined in appendix B). The surface specific humidity is simply the average of ground surface and vegetation surface specific humidities, weighted by vegetation cover,

$$q_{\text{sfc}} = \sigma_f q_f + (1 - \sigma_f) q_g. \tag{10}$$

Substituting (10) into (9) yields the partitioning of evaporation into its ground and vegetation surface components,

$$E_g = (1 - \sigma_f) \rho C_H U_a (q_g - q_a) \tag{11}$$

and

$$E_f = \sigma_f \rho C_H U_a (q_f - q_a). \tag{12}$$

Details regarding the computation of the turbulent transfer coefficient C_H and the vegetation surface specific humidity (q_f) are discussed in detail by Bosilovich and Sun (1995). In this study, the partitioned evaporative fluxes will be presented to identify the influence of various modeling strategies on the total evaporation, transpiration, and the soil evaporation.

The vegetation model should be quite important in the long-term simulation of the atmospheric surface-layer fluxes, but neither its role or its interaction with the soil parameterizations is understood. For example, Deardorff (1978) and Jacquemin and Noihlan (1990) have found sensitivity of the surface fluxes to the vegetation cover, but Wetzel and Chang (1988) and Siebert et al. (1992) find more sensitivity to the soil water content than to the vegetation cover. Furthermore, Mihailović et al. (1992) demonstrate model sensitivity to the vegetation cover when clay-type soil textures are present, but little sensitivity to vegetation when sand/loam soil types are present. Sun and Bosilovich (1996) found different sensitivities to vegetation for different soil models, and the convective PBL development was more sensitive to the initial soil moisture than soil textures for short-term (24 h) simulations. Therefore, we will also attempt to identify the impact of the vegetation model when coupled with the various soil parameterizations.

b. Experimental design

A model simulation, similar to those performed by Bosilovich and Sun (1995), has been designed to test the ability of the surface model to simulate the soil temperature, moisture, and surface energy budget for longer timescales. The duration of the simulation will be 30 days. To fulfill the objectives, model data will be compared to observations. Root-mean-square error and biases between the model simulations and the observational data will be used to quantify the model differences, as well as the model intercomparisons. Surface fluxes will be partitioned into total, daytime, and nighttime rms errors and biases. Simulations will be performed for different resolutions of the Bosilovich and Sun (1995) model. An eight-layer soil model is used to provide high resolution near the surface, where vertical moisture and temperature gradients can be very large. This will be compared to a more coarse resolution simulation (five layers). Table 2 presents the structure and initialization of the soil model.

Also, the Alpha method of computing near-surface specific humidity, proposed by Noihlan and Planton (1989), will be compared with the Deardorff (1977) Beta method in order to verify and extend (by comparing model and observed soil water) the results of Dekić et al. (1995). The FRM temperature and moisture prediction equations have been incorporated into the model and will be tested for this same case. The formulation and application of the FRM follows Deardorff. The soil moisture coefficients (C_1 and C_2) for both Deardorff (1978) and Braud et al. will be tested and compared with the observations. Another simulation for each case will examine the impact that the vegetation parameterization has on the simulation of the soil moisture, temperature, and energy budget. Table 3 provides a summary of the model simulations presented in this paper.

TABLE 3. Description and differences for each model simulation presented in this paper. All simulations use the vegetation model and beta method, unless noted otherwise.

Case	Description
1	Eight soil layers, Beta moisture availability
2	Five soil layers, Beta moisture availability
3	Eight soil layers, Alpha moisture availability
4a	Force–Restore Method, Deardorff (1978) C_1 and C_2
4b	Force–Restore Method, Braud et al. (1993) C_1 and C_2
5a	Eight soil layers, no vegetation model
5b	FRM Deardorff (1978), no vegetation model
5c	FRM Braud et al. (1993), no vegetation model

4. Results

The model is integrated for 30 days beginning at 1045 UTC 25 June 1987, which is also the beginning of IFC 2, and ending at 0000 UTC 26 July 1987. IFC 2 ends on 11 July. Figure 1 shows most of the observations used to drive the model simulation. There are several strong precipitation events that occur during this period, but most are within the first half (Fig. 1), and the second half of the period is dominated by drying during mostly cloud-free days. In general, there are warming temperatures and increasing atmospheric moisture throughout the period. There is, however, a noticeable cool and dry

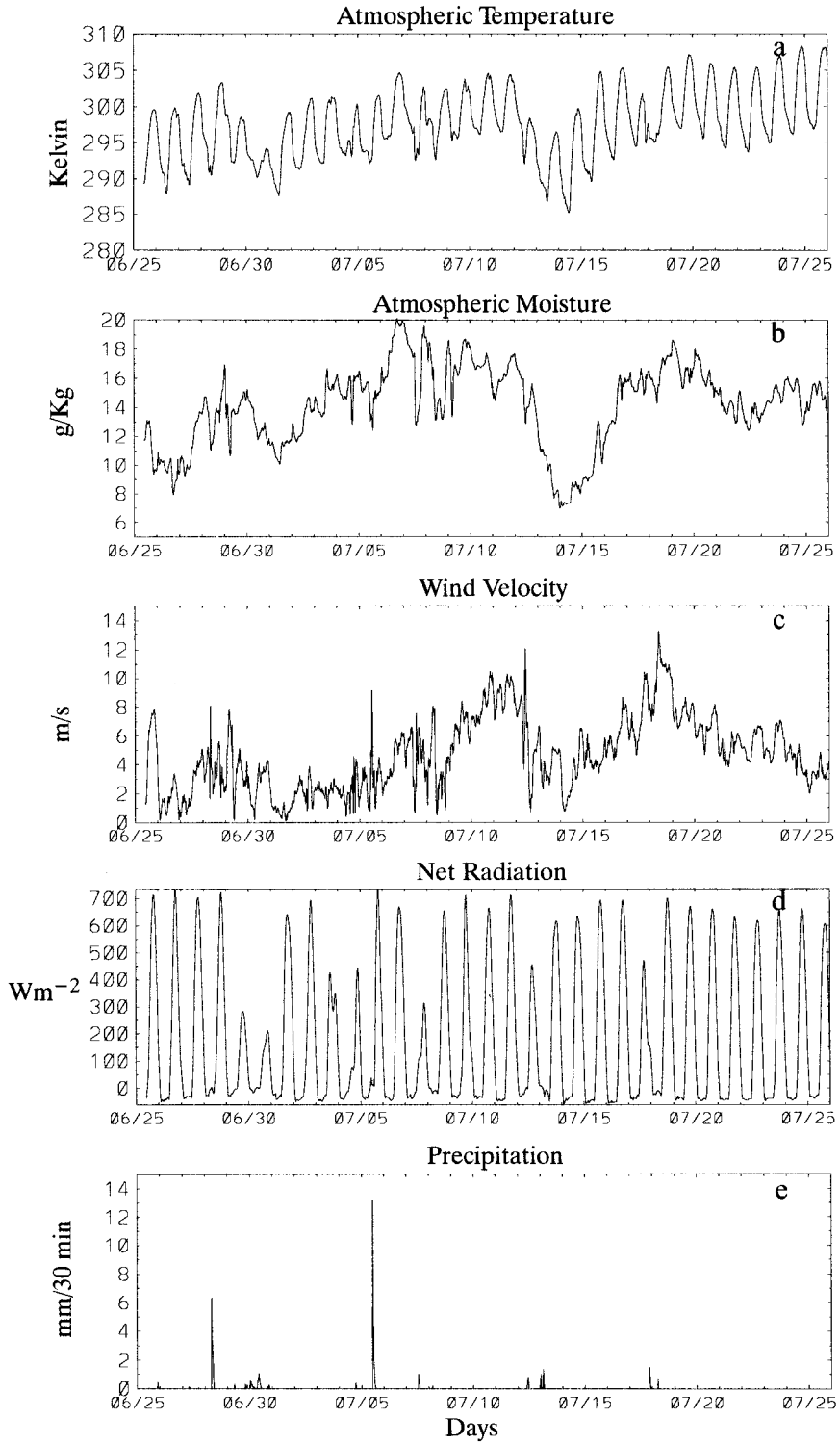

FIG. 1. FIFE site average data used as input to the model: (a) 2.0-m atmospheric temperature, (b) 2.0-m atmospheric specific humidity, (c) 5.4-m wind speed, (d) surface net radiation (computed from component radiative fluxes), and (e) precipitation rate.

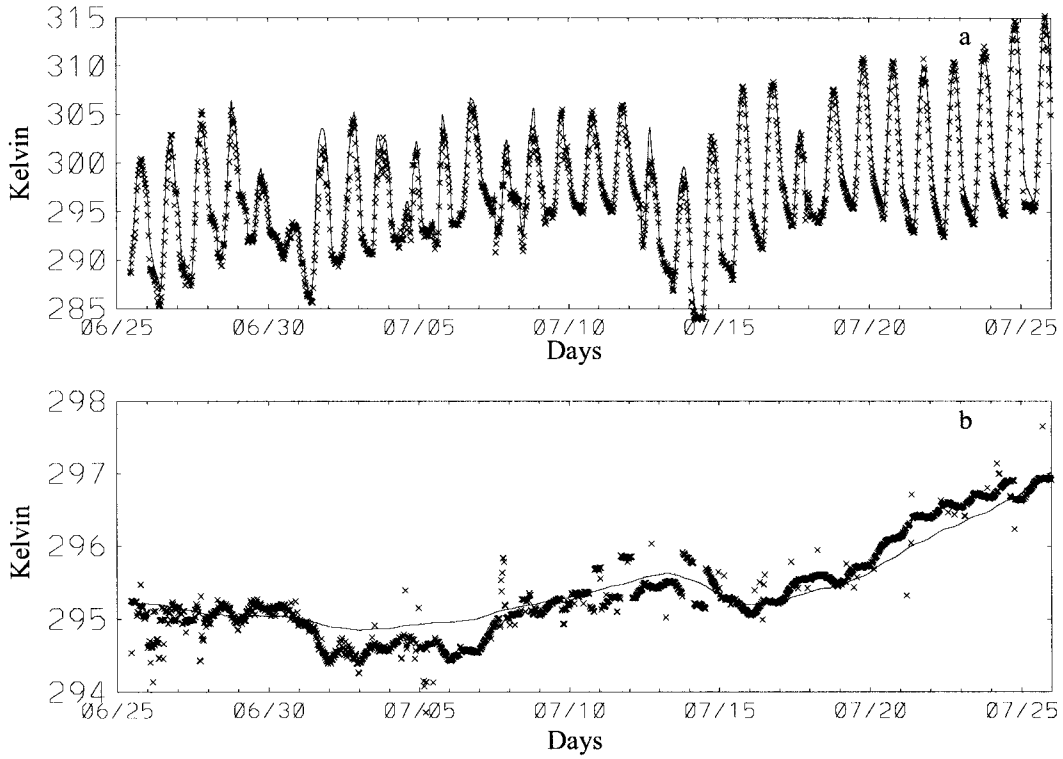

FIG. 2. Time series comparison of model-simulated (case 1) (a) surface temperature and (b) 50-cm soil temperature (solid line represents model data and crosses are observations).

period that occurs around 14 July, when a high pressure system protrudes into the FIFE region from the northwest.

a. Case 1: Eight-layer soil model

This simulation utilizes high resolution in the soil near the surface. Figure 2 shows the comparison of model-simulated surface and 50-cm temperature with observations. The model seems to follow the observed surface radiometric temperature quite well, but there is a warm bias over the whole period (Table 4). The atmospheric forcing does influence the 50-cm temperature in both the model and observation, as evidenced by the cool period that occurs in mid-July. Overall, the 50-cm soil temperature simulation seems reasonable, and the soil surface heating seems to be sufficient for the general trend of the 50-cm temperature variation. Some short-term variability in the 50-cm temperature wave is damped in the model simulation. While the thermal conductivity in the model is based on FIFE observations, there is little information below 10 cm, which, if available, could improve the model simulation.

TABLE 4. Rms error and bias (in parentheses) of model surface and 50-cm soil temperature. Note that observed surface temperature is measured by a radiometer and 50-cm soil temperature is a point observation. Units are kelvin.

Case	*T* surface	*T* at 50 cm
1	0.94 (0.83)	0.20 (0.03)
2	0.79 (0.52)	0.33 (−0.16)
3	1.14 (1.02)	0.23 (0.19)
4a	1.04 (0.93)	0.94 (0.78)
4b	0.90 (0.63)	0.61 (0.51)
5a	1.14 (0.73)	0.37 (0.35)
5b	1.84 (1.54)	1.72 (1.70)
5c	1.12 (0.02)	0.92 (0.89)

The model simulation of soil moisture is compared with observations in Fig. 3a. Note that FIFE reports only daily values of soil water (centered on 1200 UTC GMT of each day) and also that, after the end of IFC 2 (11 July), soil moisture was measured only once per week, and daily values are interpolated (Betts and Ball, 1998). The 1-m soil water comparison is quite favorable and, while the model simulation of surface soil water is quite reasonable, there are some differences. The simulated soil water is drier than observed following the large precipitation event on 5 July (Fig. 1). Betts and Ball note the possibility that precipitation could be underestimated in the observations. Also, the model soil water is slightly less than observed during the last 5–6 days of the simulation period. Figure 3b compares the simulated soil and vegetation evaporation accumulation. For this case the distribution between each component is roughly equal, despite the presence of 80% coverage of vegetation. This indicates that, in general, the model's

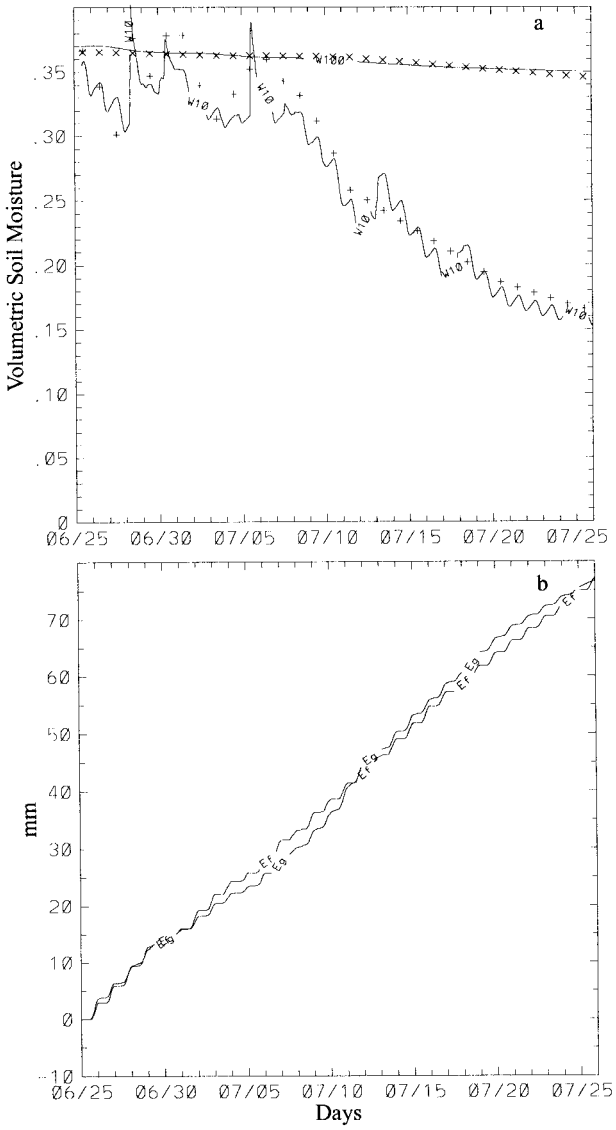

FIG. 3. Case 1 (a) comparison of model and observed soil moisture, and (b) model-simulated cumulative evaporation for the ground surface (E_g) and vegetation surface (E_t): (+) indicates observed gravimetric soil moisture for the layer 0–10 cm, and (×) indicates the neutron probe soil moisture observations at 1 m. The line marked W10 is the model 0–10-cm soil water content, and W100 is the soil water content of the layer centered at 1 m.

resistance to evaporation from the vegetation is larger than the resistance of the soil. The partitioned evaporation will be presented for each simulation, to identify the impact of different model formulations on the net and partitioned evapotranspiration.

The sign convention for the surface energy balance follows

$$R_n = H_s + LE + H_g, \tag{13}$$

where the heat fluxes are positive directed away from the surface interface (note that this is different from the convention used in most FIFE reports) and net radiation is positive directed toward the surface. Note also that surface sensible and latent heat are corrected for the component net radiation used as model input (see appendix A for more details). Scatterplots for the surface energy budget are presented in Fig. 4. In most cases, the data are evenly distributed about the 1:1 line. There is a notable exception for a model overestimate of sensible heat flux, which occurs toward the end of the simulation when the soil moisture is slightly lower than observations. Table 5 shows the total, daytime, and nighttime rms errors and bias between model and observation for each case. The accuracy of this case is within the range of error of the observing system, with the largest errors occurring generally during the daytime. Despite the underestimate of the ground heat flux, the soil temperature at 50 cm is still simulated quite well. The differences between model and observed net radiation result from upward longwave radiation differences.

b. Case 2: Coarse resolution soil

Most soil parameterizations in atmospheric numerical models use vertical resolution more comparable to that applied in this case, as opposed to the relatively high resolution (1 cm at the surface) utilized in case 1. The structure of the five-layer model in the deep soil is similar to that of case 1 (Table 2). The simulation of surface temperature improves for this case, as compared to case 1. This is due, in part, to the presence of vegetation at the surface, which can reduce the sensitivity of some soil parameters at the surface (Sun and Bosilovich 1996, and others). Other factors, addressed later in this section, also help reduce the surface temperature bias and rms error. A slight reduction in the net ground heat flux (Table 5), compared to case 1, leads to a cold bias in the 50-cm temperature simulation (Table 4). The differences between case 1 (surface soil layer 1 cm thick) and case 2 (surface soil layer 5 cm thick) occur in the partitioning of sensible and latent heat flux, as well as the ground heat flux.

The coarse model simulation of soil water content is still quite similar to the observations (Fig. 5a). The magnitude of upper-layer soil moisture toward the end of the period, however, is slightly larger than both observation and case 1. Because the surface soil layer is thicker than in case 1, the moisture available for evaporation from the ground surface is generally larger in case 2, and leads to more evaporation from the soil surface. The increase in surface evaporation helps reduce the surface temperature, which improves the surface temperature warm bias and rms error. Figure 5b, however, shows only a small difference between vegetation evaporation for case 1 and case 2 (about 4 mm over the 30-day period). The increase in soil evaporation is quite apparent in the latent heat flux bias and is coupled with a negative sensible heat flux bias (Table 5). For this case study, the five-layer simulation performs reasonably

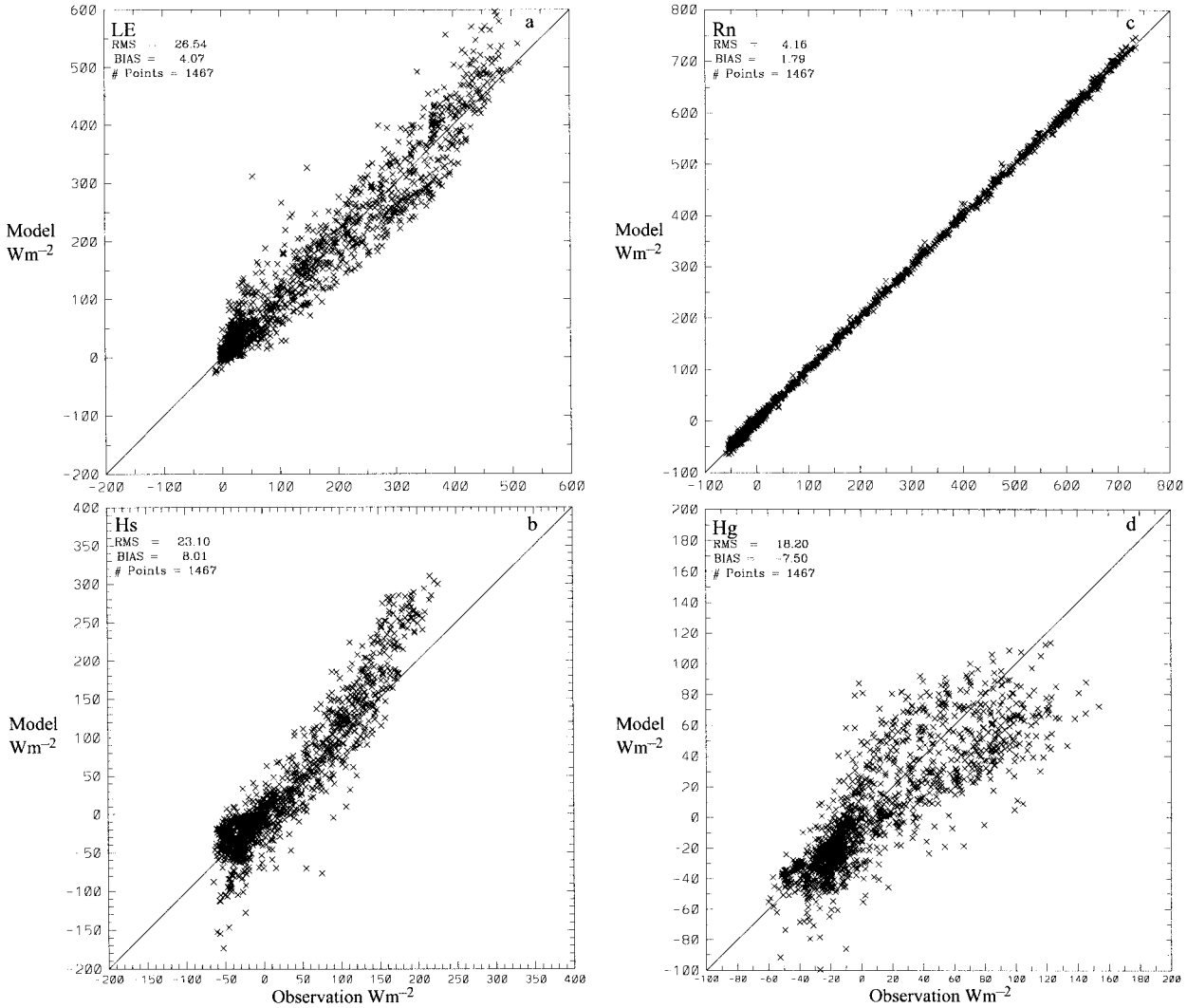

FIG. 4. Scatterplots for the case 1 surface energy budget components (a) latent heat flux, (b) sensible heat flux, (c) net radiation, and (d) ground heat flux. Units are watts per square meter.

well compared with observations. Note that other cases, where the vertical gradient of soil water is larger, may be better served by higher resolution soil models.

c. Case 3: Alpha method for moisture availability

Figure 6a shows that, during the first half of the simulation, the modeled soil moisture and evaporation are quite similar to case 1. This is expected, because the soil water content is larger than field capacity, which leads to moisture availibility in each case being close to unity [see Eqs. (1) and (2)]. Once the surface soil water content becomes less than field capacity (w_{fc} = 0.322 m^3 m^{-3} for this study), the Alpha method eventually produces more resistance to evaporation at higher values of soil water than the Beta method. Because there is more water within the soil due to the decline of ground surface evaporation, the transpiration increases for the Alpha model simulation (Fig. 6b). While the vegetation does act to reduce the differences between case 1 and case 3, there is still a net reduction of evaporation over the entire period (Table 5a). The comparison of case 3 with case 1 is similar to the results of Dekić et al. (1995); however, by incorporating the soil moisture observations we find that there is larger soil water content and less evaporation for the alpha method. Overall, the differences between case 1 and case 3 surface energy budgets are not extremely large for this time period, but the difference in soil moisture should affect the hydrology and energy budgets for very long periods (e.g., GCM simulations).

d. Case 4: Force–Restore Method

As discussed earlier, the FRM has several advantages for atmospheric numerical modeling, primarily, com-

TABLE 5. Rms error and bias (in parentheses) of model surface energy budget: (a) latent heat flux, (b) sensible heat flux, (c) net radiation, and (d) ground heat flux. Units are watts per square meter.

Case	Total	Day	Night
	(a) Latent heat flux		
1	26.54 (4.07)	34.63 (2.16)	14.54 (6.92)
2	29.22 (19.79)	38.35 (26.17)	15.69 (10.33)
3	30.41 (−4.26)	39.16 (−6.09)	17.44 (−1.54)
4a	35.29 (−7.74)	49.36 (−15.96)	14.42 (4.46)
4b	26.32 (12.98)	34.53 (16.29)	14.16 (8.09)
5a	48.91 (3.52)	70.20 (−1.85)	17.35 (11.51)
5b	84.36 (−44.32)	130.14 (−82.76)	16.42 (12.03)
5c	54.56 (45.93)	75.28 (62.76)	23.85 (20.98)
	(b) Sensible heat flux		
1	23.10 (8.01)	27.64 (11.40)	16.38 (2.96)
2	17.96 (−5.31)	19.70 (−7.90)	15.39 (−1.48)
3	26.06 (15.25)	29.49 (16.54)	21.01 (13.36)
4a	28.66 (14.35)	37.25 (21.35)	15.93 (3.97)
4b	19.56 (−1.70)	22.45 (−3.39)	15.29 (0.82)
5a	44.75 (6.63)	62.45 (8.81)	18.51 (3.40)
5b	74.97 (43.80)	113.06 (70.49)	18.44 (4.17)
5c	45.50 (−34.38)	62.51 (−54.33)	20.28 (−4.78)
	(c) Net radiation		
1	4.16 (1.79)	4.53 (2.53)	3.63 (0.69)
2	5.16 (3.67)	5.82 (4.67)	4.20 (2.19)
3	4.17 (0.81)	4.33 (2.12)	3.94 (−1.13)
4a	4.35 (1.19)	4.71 (1.67)	3.82 (0.49)
4b	4.99 (3.05)	5.58 (4.23)	4.13 (1.30)
5a	6.66 (0.00)	8.25 (0.81)	4.29 (−1.21)
5b	10.60 (−4.96)	14.53 (−7.18)	4.77 (−1.68)
5c	7.66 (4.46)	9.19 (6.99)	5.40 (0.69)
	(d) Ground heat flux		
1	18.20 (−7.50)	24.49 (−9.58)	8.88 (−4.42)
2	20.03 (−8.03)	27.63 (−12.15)	8.75 (−1.90)
3	18.70 (−7.40)	22.87 (−6.88)	12.53 (−8.19)
4a	18.42 (−2.63)	23.90 (−2.27)	10.30 (−3.18)
4b	19.44 (−5.45)	25.80 (−7.21)	10.02 (−2.85)
5a	22.97 (−7.37)	29.63 (−4.70)	13.10 (−11.34)
5b	25.94 (−1.35)	−31.97 (6.55)	17.01 (−13.11)
5c	24.07 (−4.31)	29.91 (0.01)	15.42 (−10.75)

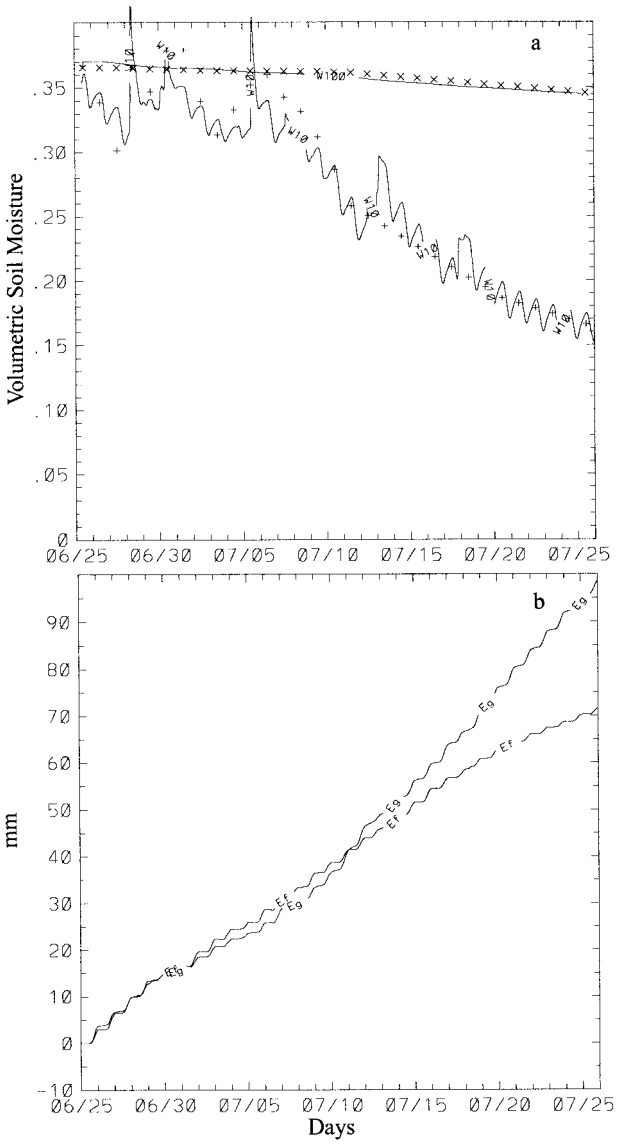

FIG. 5. As in Fig. 3 except for case 2.

putational efficiency and simple input data. For the FRM simulations, bulk soil temperature is initialized and compared with the 50-cm soil temperature observation. The FRM bulk temperature is also compared with the observed 50-cm temperature, but the model value represents a column average. Therefore, the FRM data should be used for model intercomparison rather than a strict comparison with observation. The modeled bulk soil temperature is somewhat warmer than the observations, despite the reasonable biases in ground heat flux. This is not too surprising since the bulk soil temperature represents the column average of soil temperature. On the other hand, there are differences between the two cases' simulations of soil temperature. The D78 FRM simulation produces more heat into the soil, warmer surface temperatures, and less evaporation than the B93 simulation (Tables 4 and 5).

The differences between case 4a and case 4b simulations of soil temperature and surface layer fluxes seem to be a response to each model's simulation of soil water. The D78 (case 4a) model seems quite capable during the first 10 days of the simulation, but becomes quite dry halfway through the period (Fig. 7). Ground surface evaporation is stressed during the last half of the month. The B93 simulation (case 4b), however, retains more surface soil water toward the end of the month (Fig. 8). The soil water is able to maintain the ground surface evaporation for a longer period (compared to D78).

Compared to case 1, the B93 simulation seems quite reasonable. It should be noted, however, that the depth of the bulk soil layer has some impact on the B93 simulation. Deardorff (1978), Noihlan and Planton (1989), and Braud et al. (1993) typically suggest values from 50 cm to 1 m. The depth used in this study was set at 2 m, which is similar to the depth of the case 1 and case 2 soil models. If 1 m is used in these FRM sim-

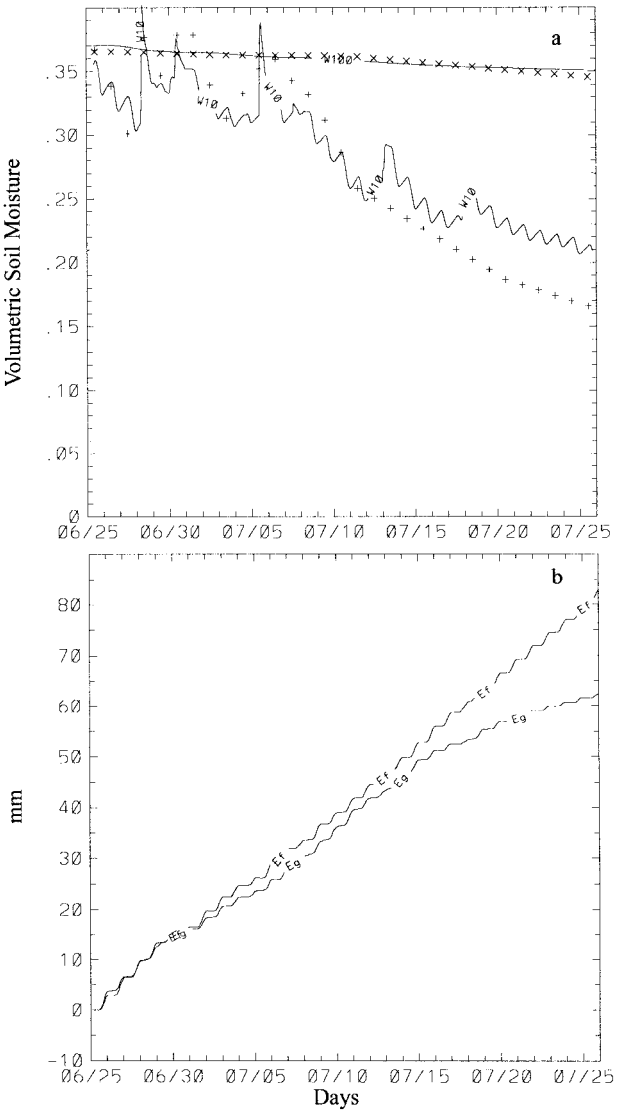

FIG. 6. As in Fig. 3 except for case 3.

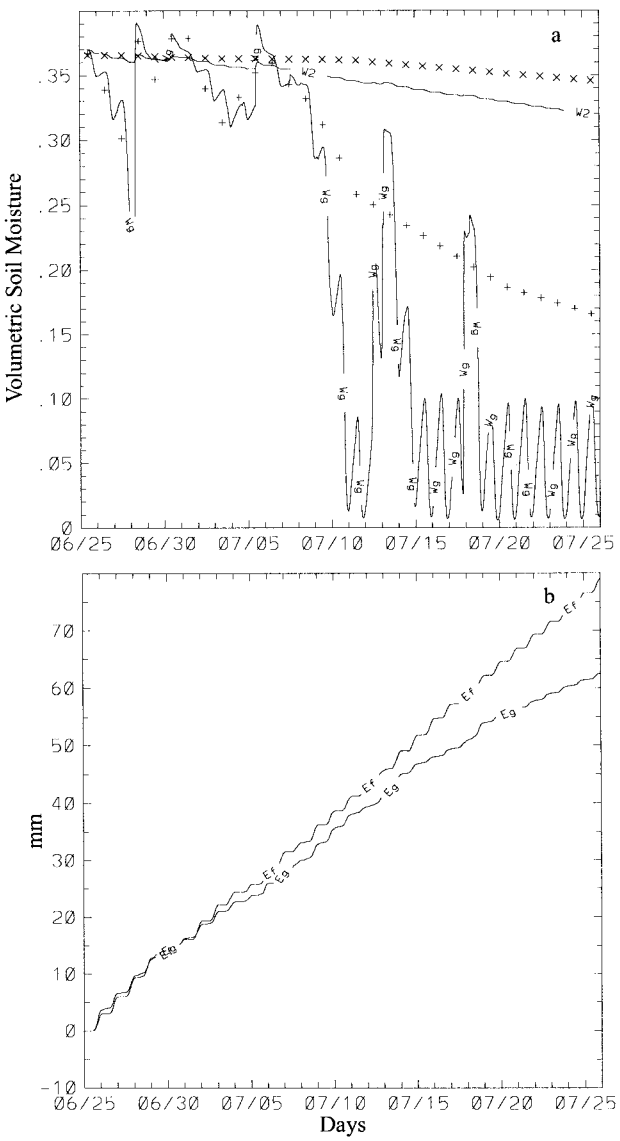

FIG. 7. Case 4a: (a) comparison of model and observed soil moisture, and (b) model-simulated cumulative evaporation for the ground surface (E_g) and vegetation surface (E_f). Note that Wg indicates the FRM surface soil water and W2 indicates the FRM bulk soil water content, neither of which are directly related to the specific FIFE observed quantity. Observations of soil water content are provided to aid in model intercomparison, (+) indicates observed gravimetric soil moisture for the layer 0–10 cm, and (×) indicates the neutron probe soil moisture observations at 1 m.

ulations (case not included in Table 5), then the surface evaporation is strongly restricted as the moisture reservoir is depleted, and the energy budget rms and bias become very unreasonable. Also, the vapor phase diffusion term in (6) is very important to the case 4b simulation of soil water. Without this term, the case 4b model simulation is more comparable to case 4a than case 1. Furthermore, the amount of water available for transpiration extends to deeper soil in the FRM simulations compared to case 1 (see Table 2). This is unavoidable in the FRM.

e. Case 5: Vegetation model

The role of the vegetation and its interaction with each case is quite different. If the vegetation model is not included in case 1, the surface soil moisture becomes somewhat drier than the simulation with vegetation and the observations (Fig. 9a). There was only a small decrease in evaporation with 147 mm cumulative in case 5a. The difference between the two cases (case 1 and case 5a) is when the evaporation occurs. Without vegetation, modeled latent heat (sensible heat) is larger (smaller) than observations during the first 10 days of the simulation and less (more) than observations during the last 10 days of simulation. This causes a low mean difference in latent heat between case 1 and 5a, but

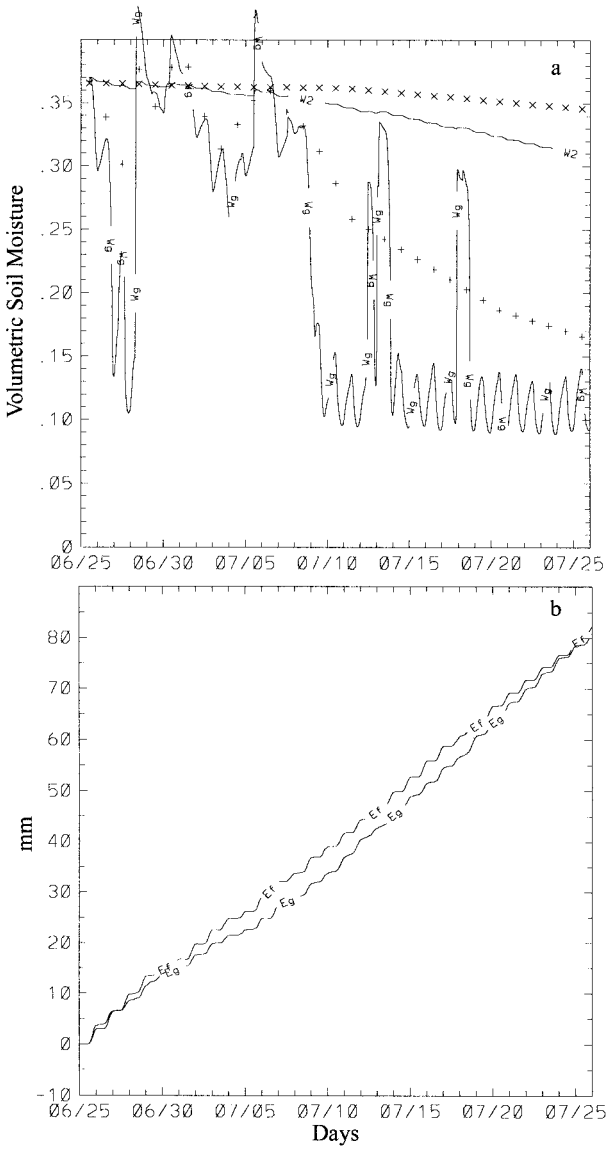

FIG. 8. As in Fig. 7 except for case 4b.

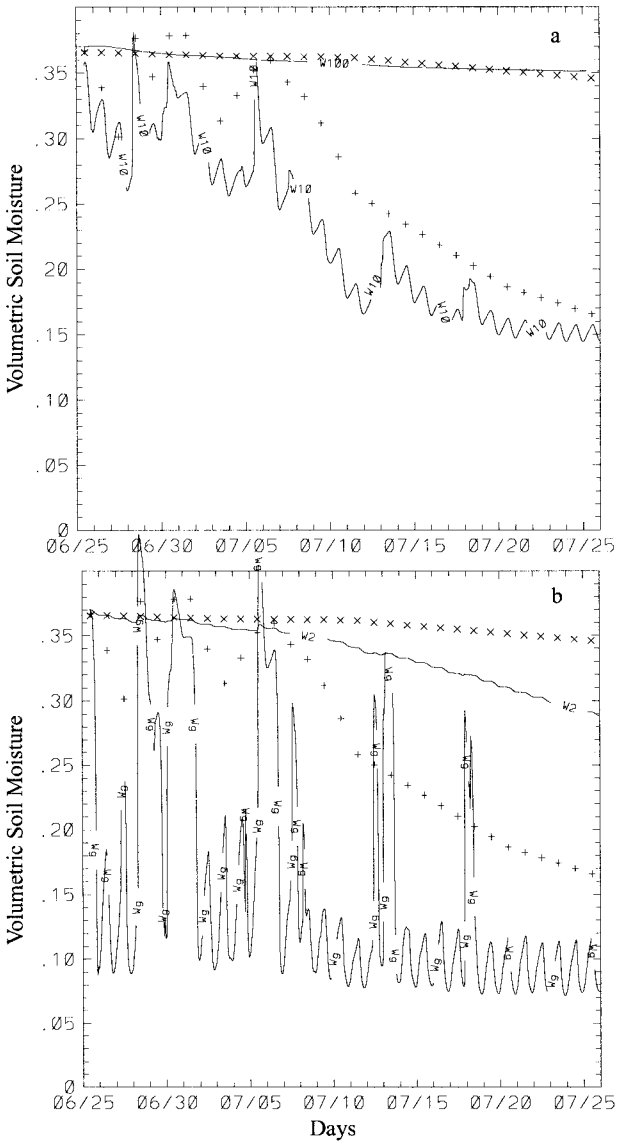

FIG. 9. (a) As in Fig. 3a and (b) as in Fig. 7a except for cases with no vegetation model, cases 5a and 5c, respectively.

larger rms error (Table 5). Therefore, with the eight-layer soil model, the vegetation acts to retard the evaporation when the soil is moist and promotes evaporation as the surface soil layers become drier. The thermal insulating effect of the vegetation is also apparent (see H_g in Table 5) where the heating of the soil is larger during the daytime and cooling is larger at night when vegetation is removed.

The two FRM cases show completely opposite responses to the removal of the vegetation. Case 5b (D78) C_1 parameterization permits surface soil water to drop to a low level, almost immediately after the simulation begins. This drastically limits the amount of surface evaporation (Table 5). Case 5c (B93) soil water content also drops considerably after initialization; however, the daily mean is larger than the D78 method. Despite the soil water being very dry (compared to observations) in Case 5c (Fig. 9b), the evaporation from the surface is much higher than observed. This shows that the vegetation model provided more resistance to the evaporation than the soil, and hence is an important source of heat for the atmosphere for case 5c. Also, the differences exhibited when comparing the cases with and without vegetation could cause fundamental problems when trying to investigate the sensitivity of GCMs to surface vegetation anomalies (e.g., deforestation).

5. Summary and conclusions

Several land surface modeling parameterizations have been examined in 30-day stand-alone simulations of the

atmospheric surface layer and soil properties. The observations used to drive and verify the model were derived from a FIFE site averaged dataset (Betts and Ball 1998) and FIFE CD-ROM (Strebel et al. 1994). Rms error and bias between model and observed surface energy budget, surface temperature, and 50-cm deep soil, as well as comparison with soil moisture, are used to verify and intercompare different land-surface parameterizations. Cumulative evaporation, partitioned into ground and vegetation components, is used to examine the interaction between the soil and vegetation models.

Increasing the model resolution did improve the model simulation of ground heat flux, especially during the daytime, which improved the modeled 50-cm soil temperature. While transpiration was similar for the high (eight layers) and coarse (five layers) resolution simulations, the ground surface evaporation was larger for the coarse resolution simulation because the thicker surface soil layer increased the availability of water. The increase in surface evaporation lowered the mean surface temperature, thereby improving the warm bias of the high resolution simulation.

The comparison of Alpha and Beta methods of moisture availability shows that during the wet period, both produce similar soil moisture and fluxes. Under drier and stressed conditions, however, the Alpha method restricts evaporation more than the Beta method. This is similar to the Dekić et al. (1995) results from a bare soil case study, except that the comparison of soil water shows that the Alpha method produces less evaporation, while the surface soil water is larger than the Beta method. This leads to a feedback with the vegetation model. Because the soil water is larger, the Alpha method transpiration is higher than the Beta method. While the mean differences between these cases were not extremely large for this particular case study (due to the combination of wet and dry periods), there is the potential for very different results from much longer simulations (e.g., GCM). The response of the different soil models to the removal of vegetation was quite variable. The variability may be an indication of uncertainty in the model simulation and sensitivity. For example, if each of these soil models were implemented in a GCM deforestation study, the results for each model could have large differences and surface/atmospheric feedbacks. To eliminate the variability, detailed observations like those of FIFE where the large amount of data greatly minimizes degrees of freedom in the model are needed for many different climatic regions and seasons.

Acknowledgments. The authors would like to thank the FIFE principal investigators and their staff for providing observational data that will be useful for many years to come. Furthermore, Drs. Alan Bett's and John Ball's considerable time in developing the FIFE site average dataset is greatly appreciated, and it will be useful in further studies. Dr. Joel Noihlan provided helpful e-mail discussions on the implementation of the Braud et al. (1993) FRM coefficients. The suggestions and comments provided by the reviewers were very useful in the final draft of this manuscript. Dr. Jiun-Dar Chern's useful discussions were invaluable to this study. We are also grateful to Mrs. Catherine Frayne for providing assistance in the preparation of the manuscript and Mr. Jim Gardner for editing the text.

APPENDIX A

Flux Correction

Kanemasu et al. (1992) and Smith et al. (1992) summarize the surface flux measurements and their uncertainties for the FIFE experiment. Field et al. (1992) find a systematic bias between net radiation measured by the component fluxes (net shortwave and net longwave measurements) and certain net radiometers. In the case of the dataset used in this study, there is a 15 W m^{-2} difference between the two forms of net radiation (time averaged over the period of this study). This leads to differences in the model and observed energy budgets, because the model requires component fluxes as input, and the observed fluxes are generally computed using (as in most of the Bowen ratio stations) the net radiometer measurements. The model energy budget is balanced by definition.

Smith et al. (1992) find that the net radiation discrepancy was most pronounced for values greater than 500 W m^{-2}, and Fritschen et al. (1992) find that Bowen ratio measurements are quite consistent and that most heat flux discrepancies result from variation in the available energy ($R_n - G$). Therefore, a correction to the sensible and latent heat flux has been applied, but only to daytime measurements. It is assumed that the Bowen ratio ($B = H_s/LE$) reported in the Betts and Ball (1998) dataset is accurate. Then, using the Bowen ratio, ground heat flux and net radiation derived from the component measurements and modified sensible and latent heat fluxes are computed. The residual of the observed energy budget (time averaged) is reduced from 15.0 W m^{-2} to 2.7 W m^{-2}. Table A1 also presents the impact the correction has on the rms error and bias for case 1.

TABLE A1. Comparison of surface and corrected surface energy budgets. The budgets have been time averaged over the period of the model simulation, and the residual of the energy budgets is also provided (see the text for sign conventions). The impact of the correction on the model rms error and bias (in parentheses) is presented. The net radiation measured by net radiometers is 165.5 W m^{-2} averaged for the period. Units are watts per square meter.

	Budget		Case 1	
	Original	Corrected	Original	Corrected
R_n	179.4	179.4	4.16 (1.79)	4.16 (1.79)
LE	135.2	145.0	31.42 (13.88)	26.54 (4.07)
H_s	19.6	22.1	24.90 (10.51)	23.10 (8.01)
H_g	9.5	9.5	18.20 (−7.50)	18.20 (−7.50)
Residual	15.1	2.8		

It should be noted that rms error for each simulation's sensible and latent heat flux was reduced using the corrected data and the results of intercomparing the different model simulations is not necessarily affected by the correction.

APPENDIX B

Symbolic Notation

B	Bowen ratio ($=H_s/LE$)
C_1, C_2	FRM soil water prediction coefficients
C_{et}	Coefficients of transpiration, analogous to root distribution
C_H	Turbulent transfer coefficient for heat and moisture
c_w	Capillary capacity (Braud et al. 1993)
D_{vh}	Diffusion of water vapor within the soil (Braud et al. 1993)
d_1, d_2	FRM thickness of the surface and bulk layers, respectively
E	Total evapotranspiration
E_f	Evaporation from the vegetation, including transpiration and evaporation of liquid water
E_g	Evaporation from the soil surface
E_{tr}	Transpiration
H_g	Ground surface heat flux
H_s	Surface sensible heat flux
h_c	Canopy height
K_1	Hydraulic conductivity (see Braud et al. 1993; Clapp and Hornberger 1978)
L	Latent heat of vaporization
LAI	Leaf area index
P_g	Precipitation rate at the soil surface
q_a	Specific humidity at the atmospheric reference level
q_g	Specific humidity of the ground surface
q_f	Specific humidity of the vegetation surface
q_{sfc}	Mean specific humidity of the surface
$q_s(T_g)$	Saturated specific humidity of the ground surface
q_*	Surface-layer scaling parameter for specific humidity
R_n	Net radiation
R_{smin}	Minimum stomatal resistance of the vegetation canopy
U_a	Reference level wind velocity
u_*	Surface-layer scaling parameter for wind velocity, also known as the friction velocity
w	In general, soil water content
w_{fc}	Field capacity soil water content
w_g	Surface layer soil water content
w_1	A limiting value of soil water (see Noilhan and Planton 1989)
w_2	Bulk layer soil water content
Z	Mean depth of a soil layer
z_{0g}	Roughness length of bare soil
ΔZ	Thickness of a soil layer
α	Alpha method moisture availability
β	Beta method moisture availability
ϵ_g	Emissivity of the soil surface
ϵ_f	Emissivity of the vegetation surface
π	The geometric constant, pi
ρ	Atmospheric density
ρ_w	Density of water
σ_f	Vegetation cover
τ_1	Diurnal period

REFERENCES

Beljaars, A. C. M., P. Viterbo, M. J. Miller, and A. K. Betts, 1996: The anomalous rainfall over the United States during July 1993: Sensitivity to land surface parameterizations and soil moisture anomalies. *Mon. Wea. Rev.*, **124,** 362–383.

Betts, A. K., and J. H. Ball, 1998: FIFE surface climate and site-averaged data set: 1987–1989. *J. Atmos. Sci.,* **55,** 1091–1108.

——, ——, and A. C. M. Beljaars, 1993: Comparison between the land surface response of the ECMWF model and the FIFE 1987 data. *Quart. J. Roy. Meteor. Soc.*, **119,** 975–1001.

Bhumralkar, C. M., 1975: Numerical experiments on the computation of ground surface temperature in an atmospheric general circulation model. *J. Appl. Meteor.*, **14,** 1246–1258.

Blackadar, A. K., 1976: Modeling the nocturnal boundary layer. *Proc. Third Symp. on Atmospheric Turbulence, Diffusion, and Air Quality*, Raleigh, NC, Amer. Meteor. Soc., 46–49.

Bosilovich, M. G., and W.-Y. Sun, 1995: Formulation and verification of a land surface parameterization for atmospheric models. *Bound.-Layer Meteor.*, **73,** 321–341.

Braud, I., J. Noilhan, P. Bessemoulin, P. Mascart, R. Haverkamp, and M. Vauclin, 1993: Bare-ground surface heat and water exchanges under dry conditions: Observations and parameterization. *Bound.-Layer Meteor.*, **66,** 173–200.

Businger, J. A., J. C. Wyngaard, Y. Izumi, and E. F. Bradley, 1971: Flux profile relationships in the atmospheric surface layer. *J. Atmos. Sci.*, **28,** 181–189.

Clapp, R. B., and G. M. Hornberger, 1978: Empirical equations for some soil hydraulic properties. *Water Resour. Res.,* **14,** 601–604.

Deardorff, J. W., 1977: A parameterization of the ground surface moisture content for use in atmospheric prediction models. *J. Appl. Meteor.*, **16,** 1182–1185.

——, 1978: Efficient prediction of ground surface temperature and moisture with inclusion of a layer of vegetation. *J. Geophys. Res.,* **83,** 1889–1903.

Dekić, L., D. T. Mihailović, and B. Rajković, 1995: A study of the sensitivity of bare soil evaporation schemes to soil wetness, using the coupled soil moisture and surface temperature prediction model, BARESOIL. *Meteor. Atmos. Phys.*, **55,** 101–112.

Dickinson, R. E., 1984: Modeling evapotranspiration for three-dimensional global climate models. *Climate Processes and Climate Sensitivity, Geophys. Monogr.,* No. 29, 58–72.

——, 1988: The force restore model for surface temperatures and its generalizations. *J. Climate,* **1,** 1086–1097.

Field, R., L. Fritschen, E. Kanemasu, E. Smith, J. Stewart, S. Verma, and W. Kustas, 1992: Calibration, comparison and correction of the net radiation instruments used during FIFE. *J. Geophys. Res.*, **97**(D17), 18 681–18 695.

Fritschen, L., P. Qian, E. Kanemasu, D. Nie, E. Smith, J. Stewart, S. Verma, and M. Wesely, 1992: Comparisons of surface flux measurement systems used in FIFE 1989. *J. Geophys. Res.*, **97**(D17), 18 697–18 713.

Garrat, J. R., 1993: Sensitivity of climate simulations to land surface and atmospheric boundary layer treatments—A review. *J. Climate,* **6,** 419–449.

Giorgi, F., G. T. Bates, and S. J. Nieman, 1992: Simulation of the

arid climate of the southern great basin using a regional climate model. *Bull. Amer. Meteor. Soc.*, **73,** 1807–1822.

Jacquemin, B., and J. Noilhan, 1990: Sensitivity study and validation of a land surface parameterization using the HAPEX-MOBILHY data set. *Bound.-Layer Meteor.*, **52,** 93–134.

Kanemasu, E., S. Verma, E. Smith, L. Fritschen, M. Wesely, R. Field, P. Kustas, H. Weaver, J. Stewart, R. Gurney, G. Panin, and J. Moncrieff, 1992: Surface flux measurements in FIFE: An overview. *J. Geophys. Res.*, **97**(D17), 18 547–18 555.

Kondo, J., N. Saigusa, and T. Sato, 1992: A model and experimental study of evaporation from bare soil surfaces. *J. Appl. Meteor.*, **31,** 304–312.

Mahfouf, J. F., and J. Noilhan, 1991: Comparative study of various formulations of evaporation from bare soil using in situ data. *J. Appl. Meteor.*, **30,** 1354–1365.

Manabe, S., 1969: The atmospheric circulation and the hydrology of the earth's surface. *Mon. Wea. Rev.*, **97,** 739–774.

Mihailović, D., H. A. R. de Bruin, M. Jeftic, and A. van Dijken, 1992: A study of the sensitivity of land surface parameterizations to the inclusion of different fractional covers and soil textures. *J. Appl. Meteor.*, **31,** 1477–1487.

Noilhan, J., and S. Planton, 1989: A simple parameterization of land surface processes for meteorological models. *Mon. Wea. Rev.*, **117,** 536–549.

Paegle, J., K. C. Mo, and J. Nogués-Paegle, 1996: Dependance of simulated precipitation on surface evaporation during the 1993 United States summer floods. *Mon. Wea. Rev.*, **124,** 345–361.

Philip, J. R., 1957: Evaporation, and moisture and heat fields in the soil. *J. Meteor.*, **14,** 354–366.

Savijärvi, H., 1992: On surface temperature and moisture prediction in atmospheric models. *Beitr. Phys. Atmos.*, **65,** 281–292.

Sellers, P. J., and J. L. Dorman, 1987: Testing the Simple Biosphere Model (SiB) using point micrometeorological and biophysical data. *J. Climate Appl. Meteor.*, **26,** 622–651.

——, Y. Mintz, Y. Sud, and A. Dalcher, 1986: The design of a Simple Biosphere Model (SiB) for use within general circulation models. *J. Atmos. Sci.*, **43,** 505–531.

——, F. G. Hall, G. Asrar, D. E. Strebel, and R. E. Murphy, 1988: The First ISLSCP Field Experiment (FIFE). *Bull. Amer. Meteor. Soc.*, **69,** 22–27.

Siebert, J., U. Sievers, and W. Zdunkowski, 1992: A one-dimensional simulation of the interaction between land surface processes and the atmosphere. *Bound.-Layer Meteor.* **59,** 1–34.

Smith, E., W. Crosson, and B. Tanner, 1992: Estimation of surface heat and moisture fluxes over a prairie grassland. 1: In situ energy budget measurements incorporating a cooled mirror dew point hygrometer. *J. Geophys. Res.*, **97**(D17), 18 557–18 582.

——, H. Cooper, W. Crosson, and W. Heng-yi, 1993: Estimation of surface heat and moisture fluxes over a prairie grassland. 3: Design of a hybrid physical/remote sensing biosphere model. *J. Geophys. Res.*, **98**(D3), 4951–4978.

Strebel, D. E., D. R. Landis, K. F. Huemmrich, and B. W. Meeson, 1994: *Collected Data of the First ISLSCP Field Experiment. Vol. 1, Surface Observations and Non Image Data Sets.* NASA, CD-ROM.

Sun, W.-Y., and J.-D. Chern, 1993: Diurnal variation of lee vortices in Taiwan and surrounding area. *J. Atmos. Sci.*, **50,** 3404–3430.

——, and M. G. Bosilovich, 1996: Planetary boundary and surface layer sensitivity to land surface parameters. *Bound.-Layer Meteor.*, **77,** 353–378.

Ungar, S. G., R. Layman, J. E. Campbell, J. Walsh, and H. J. McKim, 1992: Determination of soil moisture distribution from impedance and gravimetric measurements. *J. Geophys. Res.*, **97**(D17), 18 969–18 977.

Wang, J., 1992: An overview of the measurements of soil moisture and modeling of moisture flux in FIFE. *J. Geophys. Res.*, **97**(D17), 18 955–18 959.

Wetzel, P. J., and J. T. Chang, 1988: Evapotranspiration from a nonuniform surface: A first approach for short term numerical weather prediction. *Mon. Wea. Rev.*, **116,** 600–621.

Yee, S. Y. K., 1988: The Force Restore Method revisited. *Bound.-Layer Meteor.*, **43,** 85–90.